Rotating-frame nuclear magnetic relaxation of spins diffusing on a disordered lattice: a Monte Carlo model

1997 J. Phys.: Condens. Matter 9 9097

(http://iopscience.iop.org/0953-8984/9/42/022)

J. Phys.: Condens. Matter **9** (1997) 9097–9111. Printed in the UK PII: S0953-8984(97)85724-4

Rotating-frame nuclear magnetic relaxation of spins diffusing on a disordered lattice: a Monte Carlo model

Lu Hua†, Xiaohong Zhang and J M Titman
Physics Department, University of Sheffield, Sheffield S3 7RH, UK

Received 7 July 1997

Abstract. The rotating-frame nuclear magnetic relaxation rate of spins diffusing on a disordered lattice has been calculated by Monte Carlo methods. The disorder includes not only variation in the distances between neighbouring spin sites but also variation in the hopping rate associated with each site. The presence of the disorder, particularly the hopping rate disorder, causes changes in the time-dependent spin correlation functions which translate into asymmetry in the characteristic peak in the temperature dependence of the dipolar relaxation rate. The results may be used to deduce the average hopping rate from the relaxation but the effect is not sufficiently marked to enable the distribution of the hopping rates to be evaluated. The distribution, which is a measure of the degree of disorder, is the more interesting feature and it has been possible to show from the calculation that measurements of the relaxation rate as a function of the strength of the radiofrequency spin-locking magnetic field can lead to an evaluation of its width. Some experimental data on an amorphous metal–hydrogen alloy are reported which demonstrate the feasibility of this novel approach to rotating-frame relaxation in disordered materials.

1. Introduction

Atomic motion in disordered materials is generally characterized by a distribution of diffusion hopping or re-orientational rates. Measuring the average jump rate is relatively simple but there are very few experiments which can determine the distribution. Clearly only measuring techniques such as nuclear magnetic relaxation and neutron quasi-elastic scattering, which examine the diffusion as individual hops, are suitable. Even then the distribution can only be extracted from the experimental data if the atomic correlation function or some equivalent function is measured. The purpose of this paper is to explore the relation between the spin correlation functions and disorder in the particular case of rotating-frame nuclear magnetic relaxation by means of Monte Carlo (MC) methods and to demonstrate the experimental conditions that must be met if the degree of disorder is to be extracted from measured relaxation rates.

The high-field dipolar relaxation time, T_1, of nuclear spins diffusing on a disordered lattice has been calculated by us using MC methods and the results presented in a recent paper [1]. The intention was to provide a means of interpreting nuclear magnetic relaxation measurements of diffusion in amorphous metal–hydrogen systems in which the individual sites occupied by hydrogen atoms may have different structural and chemical environments. It was assumed that the distinguishing feature of the diffusion of the hydrogen atoms in such materials is a distribution of translational jump rates arising from the variation of

† Now at the University of Greenwich.

0953-8984/97/429097+15$19.50

binding and saddle point energies brought about by the disorder. The MC calculations showed that the time-dependent spin correlation functions were altered significantly by the presence of the jump rate distribution, particularly at high spin concentrations. In spite of the changes to the spin correlation, the disorder turned out to have relatively little effect on the temperature variation of the relaxation time, mainly because the individual jump rates behave in an Arrhenius manner and, consequently, the jump rate distribution is temperature dependent. The change in the temperature variation amounted only to a relatively modest asymmetry in the characteristic dip in T_1.

Almost all relaxation experiments on disordered metal–hydrogen alloys focus on the variation of T_1 with temperature and the MC calculations can be used to interpret such experiments in terms of the average jump rate of the spins. However, on the separate and interesting question of whether it is possible to extract the jump rate distribution from relaxation measurements the calculations imply that it is unlikely that a quantitative result concerning the jump rate distribution can be obtained from the temperature dependence of T_1 [1]. To put any value on the distribution it is clearly necessary to measure the spin correlation functions and these are not accessible in typical relaxation experiments. Given that the spectral densities of the local field fluctuations depend on the Larmor frequency, ω_0, the nearest equivalent to obtaining the spin correlation functions is to work in the frequency rather than the time domain and measure T_1 over a wide range of resonance frequency. Unfortunately, the MC calculations show that a factor of at least 100 in frequency is required in such an experiment and this is not normally feasible unless several spectrometers are available.

A rather better case can be made for measurements of the rotating-frame relaxation time, $T_{1\rho}$. In the weak-interaction approximation under those circumstances where $T_{1\rho}^{-1}$ is near its maximum value, the principal spectral density function depends not on ω_0 but on ω_1, where $\omega_1 = \gamma B_1$ and B_1 is the strength of the radiofrequency magnetic field, the spin-locking field, along which the spins relax in the rotating frame. In a typical experiment, $\omega_0/2\pi \sim 40$ MHz, $B_0 = \omega_0/\gamma \sim 10$ kG and $B_1 \sim 1$–10 G. However, it is possible to obtain radiofrequency fields of the order of 100 G by means of a suitable power amplifier, so that it may be feasible to conduct $T_{1\rho}$ experiments over a range of B_1 sufficiently wide to observe the effect of the disorder and the obtain the jump rate distribution. With this in mind we have applied the MC model described in [1] to rotating-frame relaxation in order to calculate both the radiofrequency field and temperature dependences of $T_{1\rho}$. The present paper, which is meant to be read in conjunction with our earlier paper [1], reports these calculations. They show the effect of disorder on the spin correlation functions and demonstrate the conditions under which it is possible to extract the distribution of jump rates from experimental measurements. The present calculations have been carried out for translational diffusion but the general approach adopted in them could be applied to other dynamical situations and other disordered materials in which a distribution of rates is observed.

2. The Monte Carlo simulation

Perturbation methods [2] lead to a dipolar relaxation rate in the rotating frame, $T_{1\rho}^{-1}$, given by the well known 'weak-collision' expression,

$$T_{1\rho}^{-1} = (3/8)\gamma^4\hbar^2 I(I+1)[J^{(0)}(2\omega_1) + 10J^{(1)}(\omega_0) + J^{(2)}(2\omega_0)]. \tag{1}$$

The spectral densities, J, are the Fourier transforms of the spin dipolar correlation functions $G^{(m)}(t)$, ω_0 is the Larmor frequency and ω_1 is to be regarded as a measure of the spin-locking field strength as indicated above. For present purposes $G^{(m)}(t)$ for a system with

N_s spins is defined as

$$G^{(m)}(t) = \sum_{ij} F_{ij}^{(m)} F_{ij}^{(m)*}(t)/N_s \tag{2}$$

summed over the spin pairs ij with

$$F_{ij}^{(m)}(t) = d_m Y_{2m}(\theta_{ij}, \phi_{ij}) r_{ij}^{-3} \qquad m = 0, 1 \text{ or } 2 \qquad d_2 = (32\pi/15)^{1/2} = 2d_1 = (3/2)^{1/2} d_0$$

where $Y_{2m}(\theta_{ij}, \phi_{ij})$ are normalized second-order spherical harmonics and r_{ij}, θ_{ij}, ϕ_{ij} are the polar components of the vector between the spins i and j with the z-axis parallel to B_0. The $F_{ij}^{(m)}(t)$ are random functions of time due to the fluctuations in the magnetic coupling of the nuclear spin dipoles caused by the diffusion.

The weak-collision approximation holds true when $\omega_0 \gg \omega_1$ and $\omega_1^2 \gg M_2/3$, where M_2 is the second moment of the static dipolar field distribution in frequency units. The first condition is easily met experimentally and the second is satisfied in typical metal–hydrogen systems if $B_1 \gtrsim 1$ G. Fortunately, the second condition can be relaxed when the motion of the spins is sufficiently fast that the correlation time is small compared with $M_2^{-1/2}$ [3] and it is usually possible to choose experimental temperatures which meet this criterion. In many cases it will be possible to make measurements at low spin-locking fields and it is useful to note that, in the limit of small ω_1, $T_{1\rho}$ approaches the transverse spin–spin relaxation time T_2, given by

$$T_2^{-1} = (\tfrac{3}{8})\gamma^4 \hbar^2 I(I+1)[J^{(0)}(0) + 10J^{(1)}(\omega_0) + J^{(2)}(2\omega_0)]. \tag{3}$$

Given equations (1) and (2), MC methods can be used to calculate the time variation of the spin correlation functions for a chosen degree of disorder and the relaxation rates obtained from these correlation functions by Fourier transform.

The perturbation approach of [2] is generally considered to be applicable to liquids and ordered solids. The disorder we have in mind does not shift the basic conditions of the spin system away from those in ordered solids, apart from altering the form of the correlation functions and lengthening their overall decay. In spite of the disorder there are no trapped pockets of spins which cannot escape to a different region and are not in contact with the other spins. The relaxation of spin probes which may be trapped by disorder has been discussed elsewhere [4]. In the present case we are dealing with a system of dipolar-coupled like spins which can diffuse over the whole sample. The relaxation of such spin systems has been studied by memory function methods [5], which in general lead to a non-exponential decay of the spin magnetization. It is well known that the Markovian approximation and exponential relaxation inherent in [2] are recovered for short correlation times. However it can be shown [5] that the conditions in typical high-field longitudinal relaxation (T_1) experiments are such that exponential decays of the magnetization will be observed even for correlation times greater than ω_0^{-1}. A result which is independent of the form of the correlation function and in particular true for correlation functions which can be regarded as a sum of decaying exponential functions of the type found in both the present calculations and our previous paper. The criterion, which is readily satisfied for amorphous metal hydrides, is an experimental measuring time greater than both the decay time of the correlation function and ω_0^{-1}. A similar discussion has not been given for $T_{1\rho}$ but it can easily be shown from the results given in this paper that the criterion is also satisfied when ω_0 is replaced by ω_1. Also the observed decay of the nuclear magnetization in amorphous metal hydrides is exponential in both types of measurement and the relaxation times T_1 and $T_{1\rho}$ can clearly be defined. With these features in mind we argue that the use of the perturbation formula of equation (1) is at least a satisfactory first approximation with which to demonstrate the feasibility of the $T_{1\rho}$ method.

Only a broad outline of the MC model used for these calculations is given here. The details may be found in [1]. In the MC simulation tagged spins hop on a network of sites based on a simple cubic lattice which has been distorted to approximate the structural disorder of an amorphous alloy. The distortion is produced by displacing the lattice points in random directions by up to one-third of the interatomic spacing. The restriction to one-third prevents overlap of neighbouring points. In order to jump to a neighbouring site the spins have to overcome an energy barrier which in general can be regarded as being made up of two parts, the site energy required to escape the binding force at the site and the saddle point energy, the barrier between neighbouring sites. Earlier calculations [6] have shown that, at low spin–site ratios, saddle point disorder has much less effect on the relaxation than site energy disorder, presumably because the spins almost always have a choice of diffusion paths and tend to take those with the lowest barriers. At high spin concentrations the diffusion paths are limited by site blocking and at any instant a particular spin is likely to have only one jump direction available to it. It is reasonable to suppose that the full effect of saddle point disorder will then be felt. Some unpublished calculations by one of us (JMT) based on the algorithms used in [6] indicate that, in this circumstance, changes in the spin correlation functions introduced by saddle point disorder are similar to those for site energy disorder. In contrast to this, it has been claimed that distinguishing the two types of disorder is possible through the temperature dependence of the relaxation time since the characteristic dip in the relaxation time (see figure 3) was found to be symmetric for site disorder and asymmetric for saddle disorder [7]. Our calculations do not give this result. It can be seen in the next section that the dip is clearly asymmetric for site disorder, not through any particular feature of the disorder but rather because of the temperature dependence of the individual jump rates.

As in our previous work [1] we will assume here that the saddle point energy is the same at all sites and the energy disorder is comprised solely of a random variation in the site energy. This is a conveniently simple model but, in view of the remarks above, we would argue that in the limit of very low concentration the addition of saddle point disorder, unless it is more than an order of magnitude greater than the site disorder, is of no consequence. We would also argue that it is reasonable to guess that no distinction between saddle and site disorder can be made at the highest concentration. Also the site energy distribution is assumed to be uniform between two limiting values of the energy, $E = \hat{E} \pm \delta E/2$, and the probability of a hop is taken to have the usual Arrhenius temperature dependence with a constant pre-exponential factor. This leads to a temperature-dependent distribution of jump rates given by

$$\rho(\nu) = kT/\nu\delta E = 1/n\hat{\nu}\ln(r) \tag{4}$$

where $\hat{\nu} = \nu_0 \exp(-\hat{E}/kT)$ is the hopping rate associated with the mean energy. It is important to note that in this definition the extent of the distribution can be defined by the ratio, r, of the maximum and minimum jump rates. In expression (4) $\rho(\nu)$ is normalized to unity in the interval

$$r^{-1/2} < n < r^{1/2} \qquad \nu = n\hat{\nu} \qquad r = \nu_{max}/\nu_{min} = \mathrm{e}^{\delta E/kT}. \tag{5}$$

As pointed out in the earlier paper [1] the absolute value of the jump rate $\hat{\nu}$ is not required since it enters into the relaxation rate in combination with ω_1 or ω_0. It is also convenient to introduce reduced values for the temperature T and activation energy E. The reduced temperature is defined as $\Theta = T/T_0$ and the reduced energy as $\mathcal{E} = E/kT_0$ where T_0 is the temperature at which $r = r_0$. In calculations which include the effect of changes in

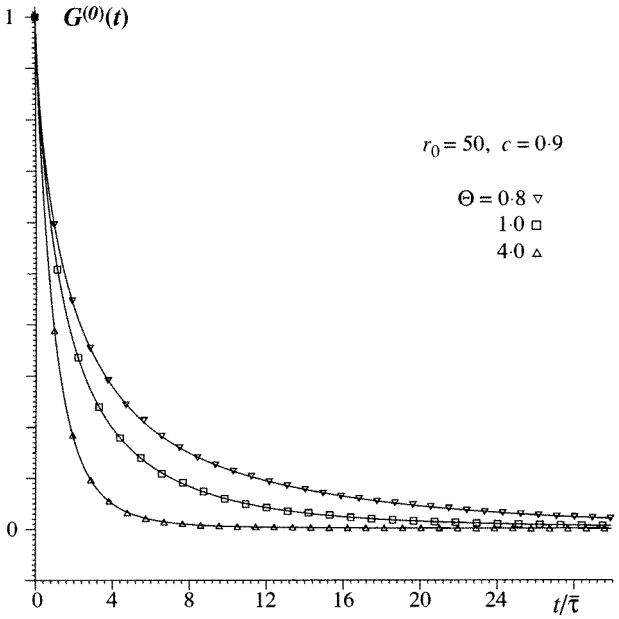

Figure 1. The normalized spin correlation function, $G^{(0)}(t)$, at various reduced temperatures, Θ, obtained from the MC calculation for a spin/site ratio of 0.9. Only a small sample of the MC data points is shown and the solid lines are the sums of five decaying exponential functions fitted to the data. The degree of disorder is represented by the parameter r as indicated in the text. It is equal to r_0 at $\Theta = 1$ and has been given a value of 50.

temperature the degree of disorder is chosen through the value given to r_0. In reduced units the jump rate distribution function becomes

$$\rho(\nu) = \Theta/n\hat{\nu}\ln(r_0) \qquad r = \exp(\delta\mathcal{E}/\Theta).$$

In order to simulate the diffusion a random number generator was used to create attempts by the spins to overcome the energy barrier and the average jump rate, $\bar{\nu}(\neq\hat{\nu})$, as a function of temperature was calculated from the attempt frequency. The spins were allowed to diffuse and the time dependences of the spin correlation functions were calculated during the diffusion for a given distribution at a chosen temperature. As indicated in [1] the actual jump rates were multiplied by a factor to keep the efficiency of the calculations approximately independent of temperature. This factor was chosen so that each data set consists of about 3000–5000 points but for clarity only a small sample is given in the figures. In order to perform the Fourier transform to the relaxation rate a sum of five decaying exponential functions were fitted to each data set. The rms deviation of the MC data from the fitted curve is typically $\sim 2\times10^{-4}$ with the deviation in any point $< 3\times10^{-3}$.

3. The temperature dependence of the relaxation rate

Figure 1 shows the time dependence of the correlation function, $G^{(0)}(t)$, normalized to its initial value. The points are samples of data from the MC calculation and the solid lines are the fitted sum of five exponential functions as indicated above. The curves demonstrate the effect of the temperature dependence of the jump rate distribution on the decay of the

correlation function. In the figure time, t, is given in units of the average interval between jumps, $\bar{\tau}$, where $\bar{\tau} = 1/\bar{\nu}$ and an increase in Θ is to be taken to imply a diminution in r due to the Arrhenius dependence of the jump rates in the model.

The general features of the correlation function are as follows. When $\Theta = 4.0$ the ratio $r = 2.7$ and $G^{(0)}(t)$ decays almost exponentially, much as it would if the system were an ordered one. The departure from exponential is due to spin–vacancy correlations which tend to reduce the decay rate at large t [1]. As the temperature is reduced and r increases the overall decay rate grows and so does the amplitude of the tail of the decay, with the result that at $\Theta = 0.8$ the ratio $r = 133$ and $G^{(0)}(t)$ departs significantly from the exponential form. $G^{(0)}(t)$ is given in figure 1 for a spin–site ratio of $c = 0.9$ and, although we do not offer any data in this paper, it can be shown that if c is reduced the overall decay rates are reduced. The effect of the reduction can be seen by reference to our earlier paper [1] for the correlation functions, $G^{(1)}(t)$ and $G^{(2)}(t)$. In fact the time, temperature and concentration dependences of $G^{(0)}(t)$ and these correlation functions are quite similar. It is for this reason that we have not reproduced any further data of $G^{(0)}(t)$ in this paper and the reader is referred to the earlier paper for the general features of the correlation functions.

A full calculation of the relaxation rate, $T_{1\rho}^{-1}$, is complicated by the presence of two variables, $\omega_1\bar{\tau}$ and $\omega_0\bar{\tau}$, which enter into the calculation when the correlation functions are Fourier transformed to find the spectral densities, J. The presence of $\bar{\tau}$ arises from the units of time in figure 1. In order to simplify the problem we need to have recourse to experiment. Firstly, as indicated above, the normal practice in experiments is to make $\omega_1/\omega_0 \ll 1$ and secondly it is usual to chose the temperature in such a way that $T_{1\rho}$ is near its minimum value for a given ω_1. Under these circumstances $\omega_1\bar{\tau}$ is of the order of unity and the term $J^{(0)}(2\omega_1)$ in equation (1) is beginning to approach its maximum (asymptotic) value, whereas $\omega_0\bar{\tau} \gg 1$ and the terms $J^{(1)}(\omega_0)$ and $J^{(2)}(2\omega_0)$ are very small. The only significant contribution to the relaxation rate then comes from $G^{(0)}(t)$. The condition is well known but can easily be ascertained by assuming that the correlation functions are decaying exponentially. The relaxation rates shown in figure 2 have been obtained with this in mind by Fourier transform of the correlation functions shown in figure 1.

The value of Θ, and therefore $\bar{\tau}$, is a different constant for each curve in figure 2. The variable on the abscissa is ω_1 and, as it approaches zero, $T_{1\rho}$ tends towards the asymptotic value T_2 as given by equation (2). For correlation functions which decay exponentially it can be shown [8] that, when the ω_0 terms are negligible, T_2^{-1} is M_2/λ, where M_2 is the frequency second moment of the static dipolar coupling. In ordered systems the decay constant, λ, is $\sim 1/\bar{\tau}$ for rapidly diffusing spins. The curve for $\Theta = 4$ corresponds to $r = 2.7$, that is not very different from the ordered state for which $r = 1$, and it can be seen from figure 1 that the decay constant of the correlation function is $\sim 1/\bar{\tau}$. The small divergence of the asymptote from unity in figure 2 is indicative of the relatively moderate departure of the correlation function from the exponential form in this case. As the width of the distribution of jump rates is increased, that is when Θ is reduced, the area under the $G^{(0)}(t)$ curve grows and with it T_2^{-1}. Figure 2 shows that, as well as its effect on $T_{1\rho}$, disorder has a significant effect on the transverse relaxation time at temperatures where the static spectrum is motionally narrowed by the rapid diffusion of the spins.

The data given in figures 1 and 2 show how the MC model can be used to calculate the temperature dependence of the relaxation rate. Applied strictly as outlined above the model gives the contribution to $T_{1\rho}^{-1}$ from the term $J^{(0)}(2\omega_1)$ in equation (1). However, in a realistic case it is necessary to consider the contributions from the other terms, which at some temperatures could become significant. When calculating the temperature dependence of the relaxation rate ω_1 and ω_0 are given constant values and $\bar{\tau}$ is a variable dependent

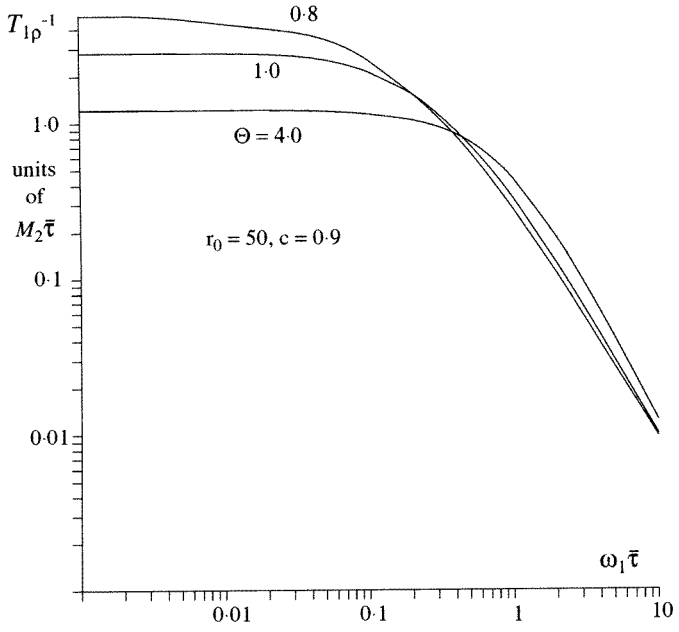

Figure 2. The relaxation rate, $T_{1\rho}^{-1}$, calculated from the correlation functions shown in figure 1. In the actual calculation of the rate, contributions from the other correlation functions were also included by setting the ratio $\omega_1/\omega_0 = 0.002$ at $2\omega_1\bar{\tau} = 1$, where $\bar{\tau}$ is the average interval between hops of the spins. In fact such contributions are negligible over the range of $\omega_1\bar{\tau}$ shown in the figure. As explained in the text $T_{1\rho}^{-1}$ approaches the asymptote T_2^{-1} at small ω_1. At $\Theta = 4$ the parameter $r = 2.7$, that is the system is close to the ordered state. In this state the value of T_2^{-1} obtained from perturbation theory is approximately $M_2\bar{\tau}$, where M_2 is the static second moment. The figure indicates that the MC calculations reduce to the theoretical value in the ordered state.

on Θ. For example, if $\Theta = 1$ is a temperature near that at which $T_{1\rho}$ is a minimum, then the relaxation rate corresponds to a value on the curve for $\Theta = 1$ in figure 2 at which $2\omega_1\bar{\tau} \sim 1$ and, as explained above, the contributions from the terms in ω_0 can be regarded as negligible. They remain negligible for lower temperatures, for example $\Theta = 0.8$ at which $2\omega_1\bar{\tau}$ is now >1 by an amount determined principally by the activation energy $\hat{E}$. On the other hand, for reasonable values of $\hat{E}$ and the ratio ω_1/ω_0, it is likely that if Θ is increased to 4, $\omega_0\bar{\tau}$ will become ~ 1 and the contributions from $J^{(1)}$ and $J^{(2)}$ will become significant.

An example of the temperature dependence of the relaxation time, $T_{1\rho}$, calculated from the MC model is shown in figure 3. In this figure ω_1 has been chosen so that $\omega_1\bar{\tau} = 1$ at $\Theta = 1$ and the reduced activation energy $\hat{E}/kT_0$ given the value 10. The data points have been calculated with the ratio ω_1/ω_0 set at 0.002 and the temperature range restricted so that the contributions from $J^{(1)}$ and $J^{(2)}$ are negligible. If ω_1/ω_0 is made 0.01 the contribution from these terms remains small over most of the temperature range but increases to about 30% near $\Theta^{-1} = 0.6$. The curves display the characteristic dip found in the dipolar relaxation time. In ordered solids ($r = 1$) the dip is symmetrical around the temperature at which $2\omega_1\bar{\tau} = 1$ as indicated by the solid curve in the figure. It can be seen that the presence of a jump rate distribution causes a shift of the minimum and the introduction of asymmetry into the dip in $T_{1\rho}$. Raising r_0 increases the asymmetry of the extreme slopes of the dip but the effect appears relatively small in view of the considerable changes in the

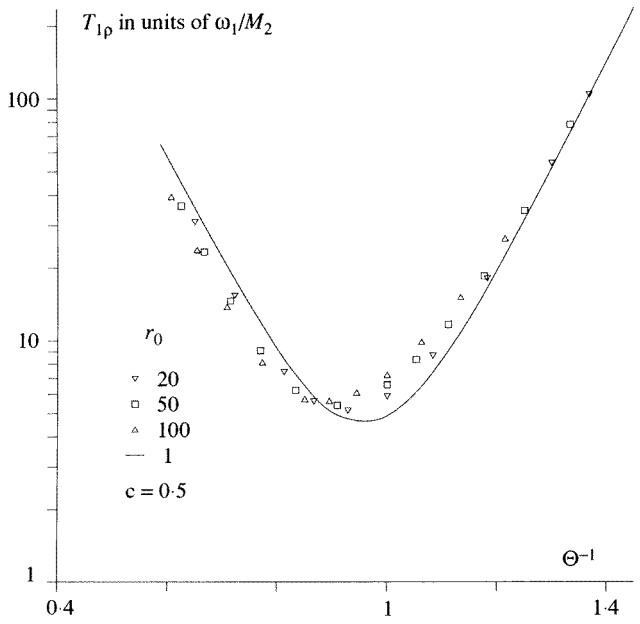

Figure 3. The dependence of $T_{1\rho}$ on reduced temperature Θ calculated from the MC simulation. As indicated in the text, the data have been calculated with the ratio ω_1/ω_0 set at 0.002 and the temperature range restricted so that $J^{(0)}$ of equation (1) is the only significant term in the relaxation rate. Data points are given for various values of r and the solid line represents the calculated relaxation time for an ordered system. The figure demonstrates that the effect of the disorder is to introduce asymmetry into the dip in $T_{1\rho}$. The minimum value $T_{1\rho}$ is close to $4\omega_1/M_2$, the theoretical value for the ordered state and exponentially decaying spin correlation functions.

correlation functions that this entails. A further addition to the asymmetry occurs because, as pointed out in the earlier paper (1), $\bar{\tau}$ does not generally have an Arrhenius dependence on temperature even though the individual jump rates do. The Arrhenius condition is only met as a special case when $c = 0.5$. Consequently, we have chosen $c = 0.5$ for the curves in figure 3 to demonstrate that asymmetry can arise solely from the effect of the jump rate distribution on the relaxation rate.

Similar features in the temperature dependence were also noted in connection with T_1 in our previous paper [1] where it was pointed out that the relatively small change in the asymmetry is a consequence of the variation of r and $\bar{\tau}$ with temperature. It can be demonstrated by reference to figure 2. The calculated values of $T_{1\rho}^{-1}$, each at a single value of $\omega_1\bar{\tau}$, trace out a locus through a family of curves of the type shown in this figure. Since these curves overlap to some extent over a large range of $\bar{\tau}$ particularly for $\omega_1\bar{\tau} > \frac{1}{2}$ the loci tend to be similar in shape at temperatures below the temperature of the $T_{1\rho}$ minimum whatever the value of r_0. This is also the case, but to a lesser extent, for higher temperatures and $\omega_1\bar{\tau} < \frac{1}{2}$ even though there are substantial differences in the magnitude of the asymptotic value. It should be noted that $T_{1\rho}^{-1}$ in figure 2 is in units of $M_2\bar{\tau}$ and it is necessary to take the change in $\bar{\tau}$ into account when translating from the locus to the temperature dependence. This has the result that $T_{1\rho}$ decreases more rapidly than $1/\bar{\tau}$ at temperatures above the minimum because the loci rise in this region as $\omega_1\bar{\tau}$ increases. At large $\omega_1\bar{\tau}$ the slopes in figure 2 are approximately -2 and at temperatures

below the minimum $T_{1\rho}$ is therefore approximately proportional to $\bar{\tau}$. The rising trend of the loci when $\omega_1\bar{\tau} < \frac{1}{2}$ is the cause of the asymmetry in the curves given in figure 3.

The MC simulation clearly predicts that the presence of a distribution of jump rates causes an asymmetry in the dip in $T_{1\rho}$ and we would argue that the results of these calculations should be used to interpret experimental data of the temperature variation of $T_{1\rho}$ in preference to simpler theoretical models [2]. It should be possible to determine the average jump rate. On the other hand one can be less sure of putting a precise value on the distribution of the jump rates from such measurements. In principle the distribution could be determined from the asymmetry but there are clearly limitations to the use of the temperature dependence for this purpose because of the weak dependence of the shape of the curves on r_0. The difficulty arises because r itself is a function of temperature and the relationship between r and $T_{1\rho}$ changes during the course of the experiment. Given that the spin correlation functions themselves are more strongly dependent on r, the implication is that only measurements made at a constant temperature are likely to lead to any meaningful estimate of the degree of disorder.

4. The dependence of $T_{1\rho}$ on the spin-locking field strength

The marked change in the spin correlation functions depicted in figure 1 shows that evaluating their time dependence should open up a possible route to ascertaining a value for r. As indicated in the introduction the spin correlation functions themselves are not generally accessible by means of relaxation measurements but the spectral density functions are, if the variation of the relaxation rate with frequency can be measured. Given the restrictions on ω_1/ω_0 and temperature mentioned above the spectral density function, $J(2\omega_1)$, and $T_{1\rho}^{-1}$ as illustrated in figure 2 are equivalent. The results in this figure are couched in terms of the temperature but as explained in the previous section they could equally well be given in terms of the distribution of jump rates. The values of r corresponding to $\Theta = 0.8$, 1 and 4 are 133, 50 and 2.7 respectively and the curves may be regarded as conveying the way in which the relaxation rate changes with r at a constant temperature.

The general appearance of figure 2 might suggest that the feature which has the most significant variation is the asymptotic value, T_2^{-1}, but of course this variation is of no value in an experiment aimed at placing a value on r. Rather than just measure T_2 it is necessary to obtain the variation of $T_{1\rho}^{-1}$ with ω_1 in order to differentiate between values of r. The difference in shape between the curves given in figure 2 can best be demonstrated by treating T_2 as a normalizing factor to bring the asymptotes into coincidence. Figure 4 gives examples of such normalized curves for which $T_{1\rho}^{-1}/T_2^{-1}$ has been calculated at a fixed temperature with $\omega_1/\omega_0 = 0.002$ at $\omega_1\bar{\tau} = 1$. In fact the ratio ω_1/ω_0 can be raised to 0.02 and cause a deviation of only 5% at the highest value of $\omega_1\bar{\tau}$ in the figure. The fact that it is easy to differentiate between the curves demonstrates that measuring $T_{1\rho}$ over a wide range of B_1 at a constant temperature is a feasible method by which the value of r could be obtained. The normalization can be achieved by measuring T_2 in a separate experiment. It should also be noted that the very wide range in the value of r is a consequence of the Arrhenius relation. It translates into a much smaller variation of the activation energy which is of course the primary feature of the disorder.

Fitting these calculated curves to experimental data requires yet another reference point and it is suggested that this could be the position at which the gradient is -1. The main reason for this choice is that this reference point can be made much clearer by plotting $\omega_1 T_{1\rho}^{-1}$ (with ω_1 in units of $1/\bar{\tau}$) rather than $T_{1\rho}^{-1}$ since the unit gradient corresponds to the

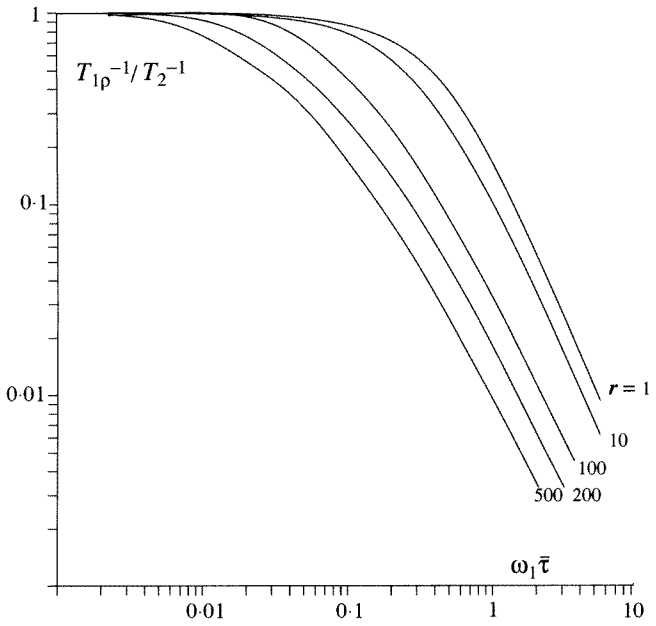

Figure 4. The relaxation rate as a function of $\omega_1\bar{\tau}$. The rate, normalized to T_2^{-1} at small $\omega_1\bar{\tau}$, was calculated at a fixed temperature with $\omega_1/\omega_0 = 0.002$ at $\omega_1\bar{\tau} = 1$ so that the only significant contribution comes from the spectral density $J^{(0)}$. The effect of changing the ratio ω_1/ω_0 is indicated in the text. The curves reflect the marked change in the spectral densities introduced by the disorder.

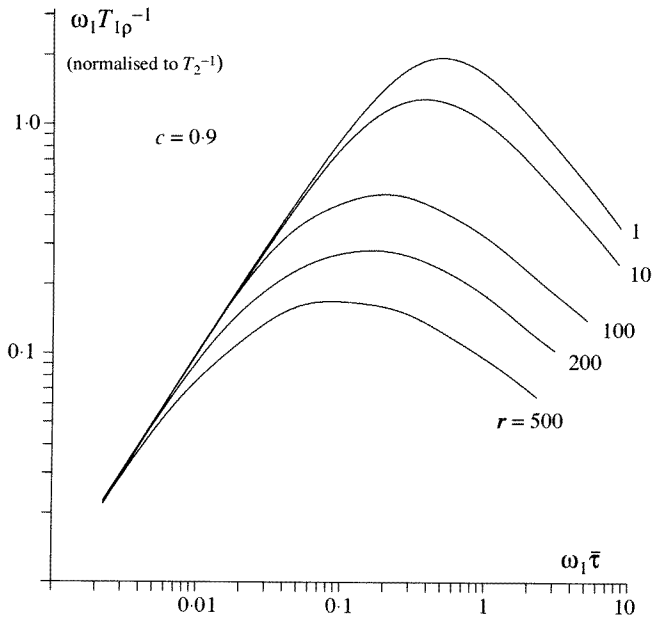

Figure 5. As indicated in the text the product $\omega_1 T_{1\rho}^{-1}$ rather than $T_{1\rho}^{-1}$ itself is more useful in interpreting experimental results. The data of figure 4 are plotted as $\omega_1 T_{1\rho}^{-1}$ in the figure with ω_1 in units of $1/\bar{\tau}$ and $T_{1\rho}^{-1}$ normalized by T_2^{-1}.

maximum of $\omega_1 T_{1\rho}^{-1}$ in the new plot. The MC data of figure 4 are repeated in this new form in figure 5. Of course, when fitting to experimental data it will not be possible to distinguish between the maxima in $\omega_1 T_{1\rho}^{-1}$ and a more realistic comparison between the curves requires yet another re-normalization to the same maximum value. To visualize this effect it is necessary to imagine the curves slid along the line with unit gradient corresponding to the $T_{1\rho} = T_2$ asymptote. An example is shown in figure 6 where data are furnished for $c = 0.5$ rather than 0.9 to give some indication of the range of our calculations. Data of the form given in figure 6 appear to be the most useful when fitting to experiment. In an experiment, given the typical parameters quoted above, B_1 could range from, say, 1 to 100 G, which with a judicious choice of $\bar{\tau}$ (or T) could cover the whole of the peak in figure 6 from $\omega_1\bar{\tau} = 0.1$ to 10. Depending on the experimental situation, it may also be necessary to have motional narrowing in order to relax the conditions for the weak-collision approximation for $T_{1\rho}$.

In order to make use of the MC calculations it is necessary to have data on $T_{1\rho}^{-1}$ or $J^{(0)}(2\omega_1)$ in the form given in figures 4, 5 or 6. Just as the spin correlation functions can be fitted by the sum of five exponentials the spectral density functions can be fitted by the sum of five Lorentzian functions. The appendix gives tables of parameters based on this fitting procedure which can be used to generate $J^{(0)}(2\omega_1)$ for a wide range of c and r. The resulting spectral density functions are in the form shown in figure 4, that is normalized to unity at $\omega_1 = 0$. Any contributions to the relaxation rate from the spectral density functions involving ω_0 will usually be small and can be obtained to a fairly good approximation by assuming that the normalized functions $J^{(0)}(2\omega_1)$, $J^{(1)}(\omega_0)$ and $J^{(2)}(2\omega_0)$ are the same apart from the change of variable.

5. Comparison with experiment

In order to make contact with experiment we have made measurements of the hydrogen spin-locked relaxation time in an amorphous Zr_2Pd–H alloy. Binary transition metal alloys are known to have a distribution of hydrogen binding energies from electrochemical measurements [9] and there is evidence from internal friction experiments of a distribution of hydrogen activation energies [10, 11]. The exact form of the energy disorder is not known, especially the division between saddle and site energies. The computer model includes the main feature, a distribution of binding energies, and it may be regarded as, a least, a first approximation to an actual metal–hydrogen system.

The sample was made by first melting the metal components in an argon arc furnace and then melt spinning to obtain amorphous Zr_2Pd. The hydrogen was added by immersing the sample in hydrogen gas at a pressure of 1 bar and a temperature of 150 °C to produce the alloy $Zr_2PdH_{3.3}$. The aim of this experiment was not to obtain the temperature dependence of the relaxation rate but to measure $T_{1\rho}$ at a fixed temperature (295 K) over a wide range of spin-locking field B_1 ($\leqslant$35 G). It was carried out because, as far as we were aware, no measurements involving a sufficiently wide range of B_1 had been conducted previously. The data points in figure 7 are the values of $\omega_1 T_{1\rho}^{-1}$ obtained from the experiment, the value of ω_1 and the spin-locking field at each measurement being determined from the length of the spin-locking rf pulse required to cause the nuclear magnetization to precess through the angle π. In addition T_2 was determined to be 35 ± 2 μs from the free induction decay following a $\pi/2$ pulse.

The solid curves in the figure are calculated from the MC simulation. They have been adjusted to the experimental value of T_2 at small ω_1 and their maxima were chosen to coincide with the data. The quality of the data makes it difficult to place a precise value on r and for the figure we have simply chosen one of our calculated curves (for $c = 0.9$)

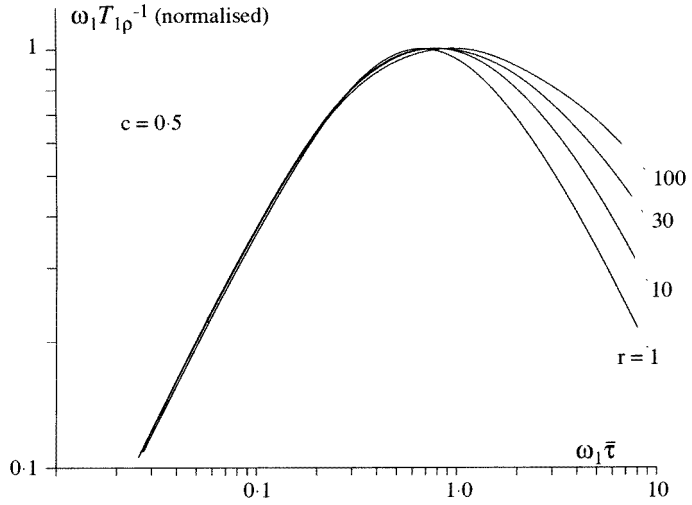

Figure 6. The product $\omega_1 T_{1\rho}^{-1}$ plotted as a function of $\omega_1\bar{\tau}$ for a spin/site ratio of 0.5. The form of the curves differs from those of figure 5 in that the data have been normalized by the maximum value of $\omega_1 T_{1\rho}^{-1}$. In experiments the value of T_2 is assumed to be measured but the value of $\omega_1\bar{\tau}$ at the maximum is not usually known. A true comparison of the curves thus entails not only normalizing them but also shifting them along the line with unit gradient corresponding to the $T_{1\rho} = T_2$ asymptote. Consequently, the abscissa gives the true value of $\omega_1\bar{\tau}$ only for $r = 1$. In spite of this treatment the curves still show significant changes as r is altered.

which gives a reasonable fit. Nevertheless, it is quite clear that the curve for $r = 1$ does not fit the data. Thus, in keeping with the main aim of the experiment, we have established that the MC calculations can be applied to amorphous systems and that there are features of the relaxation which can be interpreted by a distribution of activation energies. The average interval between diffusion hops, $\bar{\tau}$, can be calculated from the fitting procedure to be 6.7×10^{-7} s and the spread in activation energy corresponding to $r = 500$ is ± 0.079 eV. The reason for choosing the temperature of 295 K is that it is known from previous work on the temperature dependence of the relaxation in amorphous Zr_2Pd–H that $T_{1\rho}$ is a minimum at ~300 K when $B_1 = 7$ G [12]. In the earlier work the minimum value of $T_{1\rho}$ is 230 μs which compares well with 275 μs in the present work at the same spin-locking field. The samples are not identical in that they have slightly different hydrogen to metal atomic ratios. The equivalent of $\bar{\tau}$ in the earlier work was found to be 17×10^{-7} s but it is not expected that the values will coincide since the methods of evaluation are entirely different.

In the earlier work [12] attention was drawn to the fact that the dip in the $T_{1\rho}$–T experimental curve is not symmetrical and this was explained on the basis of standard relaxation models as a change in the activation energy from 0.21 eV at low temperatures to 0.43 eV at high temperatures. An unusual feature of the data was that this change in activation energy occurred at a temperature near to, but somewhat higher than, the temperature of the minimum. It was not possible to give a physical interpretation of this coincidence or the change in activation energy. The present work offers a different explanation for the asymmetry found in the experiment, namely the presence of a distribution of jump rates. By making $T_0(\Theta = 1)$ equal to 270 K the minima in the curves in figure 3 occur at ~300 K and the activation energy $\hat{E}$ turns out to be 0.23 eV. The ratio the apparent activation energies above and below the $T_{1\rho}$ minimum is 1.4 for the $r_0 = 100$ curve and, of course, the change in activation energy occurs at a temperature where $T_{1\rho}$ is near its

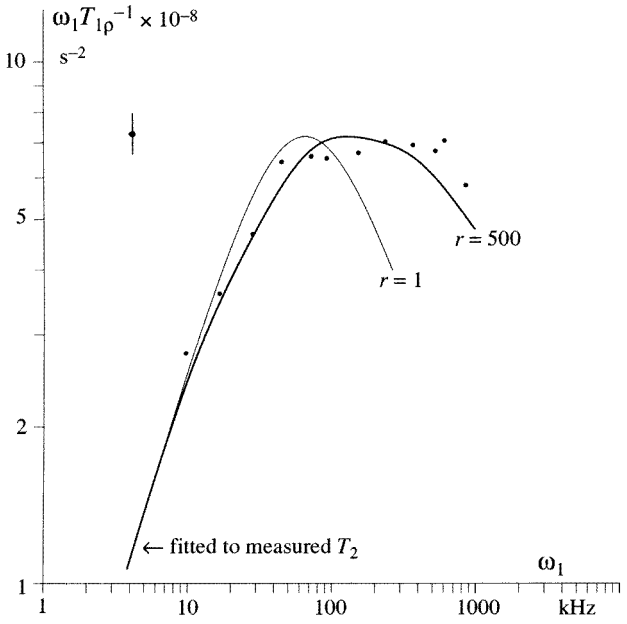

Figure 7. The data points are experimental values obtained for the amorphous alloy $Zr_2PdH_{3.3}$ as described in the text, a typical error bar being indicated by the displaced point to the left of the peak. The solid curves were calculated from the MC simulation. They have been adjusted to the experimental value of T_2 at small ω_1 and their maxima were chosen to coincide with the experimental data. They are therefore related to each other in the manner given in figure 6. The presence of disorder in the sample is clearly demonstrated.

minimum. A greater value of the ratio than this could be obtained if the value of r_0 were raised. The MC calculations can thus be made to explain the difference in slope of the experimental $T_{1\rho}$–T relationship at the extremes of the dip. Unfortunately, fitting the whole of the experimental data is not possible, since calculation and measurement do not agree over the full range of the measurements. The shape of the calculated relaxation curves close to the minimum is significantly different from that found in the experiment. It is clear from our work that making calculations with a greater r_0 will not remove this divergence.

These measurements are to be regarded as preliminary to a fuller investigation and are given merely to establish the feasibility of the method. Nevertheless it is necessary to show that they were made under the weak-collision approximation of the original theoretical expressions. The condition that $\omega_0 \gg \omega_1$ is easily met since even at the maximum value of ω_1 the ratio ω_0/ω_1 was always greater than 150. The other condition, that $\omega_1^2 \gg M_2/3$, cannot be satisfied for all values of ω_1. Assuming that the relaxation rate of 275 μs given above represents the minimum $T_{1\rho}$, the second moment may be obtained from the MC data given in figure 3. The value is 3.4×10^{-3} μs^{-2} which is comparable with $M_2 = 5.35 \times 10^{-3}$ μs^{-2} obtained from earlier measurements on a slightly different sample [13]. Thus $\omega_1^2 \gg M_2/3$ is reasonably well satisfied for about half the experimental data points but it cannot be true as the T_2 asymptote is approached. The temperature 295 K was also chosen for the experiment because it is high enough to cause substantial motional narrowing of the resonance line and therefore eases this restriction. That motional narrowing has occurred can be seen to be the case since the spin correlation time, which is approximately equal to $\bar{\tau}$, is about one order of magnitude smaller than $M_2^{-1/2}$.

6. Summary

MC calculations of the spin-locked relaxation rate, $T_{1\rho}^{-1}$, in a diffusing spin system characterized by a distribution of jump rates have been made. The results show that the variation of $T_{1\rho}^{-1}$ with the strength of the rf spin-locking magnetic field, B_1, depends on the distribution. The dependence is sufficiently strong to demonstrate that making measurements at a constant temperature with B_1 as a variable can lead to an evaluation of the degree of disorder. The feasibility of carrying out such an experiment is supported by measurements.

Acknowledgment

The authors are grateful for a grant from the Engineering and Physical Sciences Research Council in support of this work.

Appendix

The spectral densities $J^{(0)}$ may be calculated as a function of $\omega_1\bar{\tau}$ from the data given. $J^{(0)}$ is the sum of five terms of the form $ab/[b^2 + (\omega_1\bar{\tau})^2]$, where a and b are given as pairs in the tables. The parameters r and c are those in the main text.

Table A1.

r						
$c = 0.3$						
1	a	0.395 88	0.141 12	$1.272\,11 \times 10^{-2}$	$1.381\,76 \times 10^{-2}$	$1.418\,26 \times 10^{-3}$
	b	0.852 44	0.383 53	0.116 94	4.381 37	$2.546\,46 \times 10^{-2}$
20	a	−0.636 13	0.178 96	0.807 23	$3.080\,75 \times 10^{-2}$	$1.076\,81 \times 10^{-3}$
	b	1.109 97	0.312 45	1.109 97	0.131 29	$2.787\,28 \times 10^{-2}$
50	a	$7.934\,23 \times 10^{-2}$	0.145 44	$6.497\,44 \times 10^{-3}$	$6.537\,05 \times 10^{-2}$	$5.369\,32 \times 10^{-4}$
	b	1.587 09	0.389 48	$9.185\,16 \times 10^{-2}$	0.135 75	$2.165\,89 \times 10^{-2}$
200	a	$4.892\,15 \times 10^{-2}$	$8.750\,06 \times 10^{-2}$	$9.694\,50 \times 10^{-2}$	$-2.862\,75 \times 10^{-2}$	$1.786\,92 \times 10^{-3}$
	b	1.397 28	0.328 70	0.106 10	0.106 10	$3.222\,24 \times 10^{-2}$
300	a	$9.504\,60 \times 10^{-3}$	$2.374\,63 \times 10^{-2}$	$7.472\,88 \times 10^{-2}$	$7.674\,08 \times 10^{-2}$	$7.960\,39 \times 10^{-4}$
	b	6.707 10	1.475 24	0.100 79	0.402 72	$1.530\,30 \times 10^{-2}$
500	a	$4.793\,64 \times 10^{-2}$	$2.684\,57 \times 10^{-2}$	$4.587\,25 \times 10^{-2}$	$2.157\,50 \times 10^{-2}$	$1.173\,37 \times 10^{-2}$
	b	0.778 76	0.278 17	$8.668\,74 \times 10^{-2}$	0.188 56	$5.893\,27 \times 10^{-2}$
$c = 0.5$						
1	a	7.46933×10^{-2}	0.173 38	$1.329\,69 \times 10^{-2}$	0.278 38	$7.015\,10 \times 10^{-4}$
	b	1.772 51	0.396 23	$0.106\,23 \times 10^{-2}$	0.773 63	$1.988\,35 \times 10^{-2}$
20	a	0.128 04	0.155 67	0.243 65	−0.181 11	$3.039\,03 \times 10^{-3}$
	b	0.340 34	1.099 94	0.171 51	0.179 52	$4.295\,47 \times 10^{-2}$
50	a	−0.263 70	$7.144\,76 \times 10^{-2}$	$7.967\,81 \times 10^{-2}$	0.382 07	$1.625\,80 \times 10^{-3}$
	b	0.404 22	1.703 55	0.129 37	0.404 22	$3.293\,86 \times 10^{-2}$
200	a	$2.847\,02 \times 10^{-2}$	$6.189\,98 \times 10^{-2}$	$2.148\,61 \times 10^{-2}$	$6.127\,77 \times 10^{-2}$	$1.615\,33 \times 10^{-5}$
	b	2.758 38	0.490 43	$5.505\,14 \times 10^{-2}$	0.129 59	$4.871\,29 \times 10^{-2}$
300	a	$2.338\,51 \times 10^{-2}$	$5.822\,14 \times 10^{-2}$	$2.992\,50 \times 10^{-2}$	$4.896\,85 \times 10^{-2}$	$-1.272\,33 \times 10^{-2}$
	b	2.788 95	0.124 26	$3.460\,59 \times 10^{-2}$	0.488 49	$2.879\,31 \times 10^{-2}$
500	a	$4.004\,76 \times 10^{-2}$	$1.333\,28 \times 10^{-2}$	$2.691\,97 \times 10^{-2}$	$2.468\,26 \times 10^{-2}$	$2.073\,33 \times 10^{-4}$
	b	0.159 25	2.543 01	$5.082\,70 \times 10^{-2}$	0.631 20	$1.170\,38 \times 10^{-3}$

Table A2.

r						
$c = 0.7$						
1	a	0.106 20	−1.122 53	$3.107\,68 \times 10^{-2}$	1.474 99	$1.716\,10 \times 10^{-3}$
	b	1.692 62	0.524 99	0.150 32	0.524 99	$2.901\,84 \times 10^{-2}$
20	a	$-2.345\,96 \times 10^{-2}$	0.163 26	$6.813\,60 \times 10^{-2}$	$9.285\,36 \times 10^{-2}$	$1.237\,82 \times 10^{-3}$
	b	0.260 03	0.364 93	0.133 44	1.189 70	$2.290\,61 \times 10^{-2}$
50	a	$5.558\,93 \times 10^{-2}$	$7.325\,00 \times 10^{-2}$	$4.966\,88 \times 10^{-2}$	$4.918\,72 \times 10^{-2}$	$1.468\,89 \times 10^{-3}$
	b	1.645 04	0.438 74	$9.946\,02 \times 10^{-2}$	0.206 35	$2.384\,52 \times 10^{-2}$
200	a	$1.874\,30 \times 10^{-2}$	$4.801\,27 \times 10^{-2}$	$3.018\,59 \times 10^{-2}$	$3.260\,55 \times 10^{-2}$	$3.782\,45 \times 10^{-4}$
	b	0.385 00	0.175 75	$4.993\,83 \times 10^{-2}$	1.483 84	$7.294\,47 \times 10^{-3}$
300	a	$-9.564\,11 \times 10^{-2}$	$3.093\,10 \times 10^{-2}$	$7.163\,97 \times 10^{-2}$	$8.388\,35 \times 10^{-2}$	$1.463\,43 \times 10^{-2}$
	b	0.149 39	0.934 76	0.106 21	0.193 36	$2.934\,04 \times 10^{-2}$
500	a	$2.809\,38 \times 10^{-2}$	$2.719\,17 \times 10^{-2}$	$-8.768\,09 \times 10^{-3}$	$2.575\,58 \times 10^{-2}$	$1.303\,84 \times 10^{-2}$
	b	$6.042\,50 \times 10^{-2}$	0.782 40	$4.281\,42 \times 10^{-2}$	0.162 34	$2.386\,24 \times 10^{-2}$
$c = 0.9$						
1	a	$6.877\,11 \times 10^{-2}$	0.338 32	$3.480\,91 \times 10^{-2}$	$-1.789\,62 \times 10^{-2}$	$3.697\,02 \times 10^{-3}$
	b	1.456 51	0.467 22	0.170 25	0.321 68	$4.630\,90 \times 10^{-2}$
20	a	$6.661\,33 \times 10^{-2}$	0.315 05	$5.452\,31 \times 10^{-2}$	−0.190 99	$2.850\,47 \times 10^{-3}$
	b	1.128 42	0.308 15	0.122 36	0.308 15	$3.051\,26 \times 10^{-2}$
50	a	$8.563\,39 \times 10^{-3}$	$7.942\,07 \times 10^{-2}$	$5.510\,77 \times 10^{-2}$	$2.482\,16 \times 10^{-2}$	$7.916\,81 \times 10^{-3}$
	b	6.408 34	0.355 84	0.103 30	1.429 93	$3.523\,73 \times 10^{-2}$
200	a	$3.181\,22 \times 10^{-2}$	$1.707\,81 \times 10^{-2}$	$2.561\,60 \times 10^{-2}$	$6.735\,12 \times 10^{-3}$	$5.098\,93 \times 10^{-3}$
	b	0.251 41	1.219 39	$7.390\,77 \times 10^{-2}$	$2.470\,52 \times 10^{-2}$	$2.074\,50 \times 10^{-2}$
300	a	$8.483\,93 \times 10^{-3}$	$1.577\,07 \times 10^{-2}$	$2.751\,41 \times 10^{-2}$	$1.560\,61 \times 10^{-2}$	$1.987\,19 \times 10^{-3}$
	b	$1.756\,98 \times 10^{-2}$	0.245 39	$7.847\,21 \times 10^{-2}$	0.613 17	$2.586\,81 \times 10^{-2}$
500	a	$5.093\,59 \times 10^{-3}$	$7.339\,33 \times 10^{-3}$	$2.170\,88 \times 10^{-2}$	$1.500\,48 \times 10^{-2}$	$6.003\,46 \times 10^{-3}$
	b	0.478 30	2.022 36	$5.486\,82 \times 10^{-2}$	0.227 24	$1.145\,56 \times 10^{-2}$

References

[1] Lu Hua, Titman J M and Havill RL 1995 *J. Phys.: Condens. Matter* **7** 7501
[2] Look D C and Lowe I J 1966 *J. Chem. Phys.* **44** 2995
[3] Ailion D 1971 *Adv. Magn. Res.* **5** 172
[4] Borg P, Kehr K W and Heitjans P 1995 *Phys. Rev.* B **52** 6668
[5] Diezemann G and Schirmacher W 1990 *J. Phys.: Condens. Matter* **2** 6681
[6] Crouch M A Havill R L and Titman J M 1986 *J. Phys. F: Met. Phys.* **16** 99
[7] McDowell A F and Cotts R M 1994 *Z. Phys. Chem.* **183** 65
[8] Abragam A 1961 *The Principles of Nuclear Magnetism* (Oxford: Clarendon)
[9] Harris J H, Curtin W A and Tenhover M A 1987 *Phys. Rev.* B **36** 5784
[10] Berry B S and Pritchet W C 1981 *Phys. Rev.* B **24** 2299
[11] Hazelton L E and Johnson W L 1984 *J. Non-Cryst. Solids* **61/62** 667
[12] Bowman R C Jr, Cantrell J S, Attalla A, Etter D E, Craft B D Wagner J E and Johnson W L 1984 *J. Non-Cryst. Solids* **61/62** 649
[13] Kemali M, Havill R L and Titman J M 1995 *Phil. Mag.* B **72** 275